Preparation and Surface Effect Analysis of Trivalent Europium-Doped Nanocrystalline La_2O_2S

Hongshang Peng,*,† Shihua Huang,† Fangtian You,† Jianjun Chang,† Shaozhe Lu,‡ and Lin Cao§

Institute of Optoelectronic Technology, Beijing Jiaotong University, 100044 Beijing, China, Key Laboratory of Excited-State Physics, Chinese Academy of Science, Changhcun, China, and University of Science and Technology, Beijing, Beijing, China

Received: October 12, 2004; In Final Form: December 22, 2004

$La_2O_2S:Eu^{3+}$ nanocrysytals (NCs) with a mean size of 18 nm are prepared by gel thermolysis. The morphology of the particles is hexagonal. The surface Eu^{3+} ions are first detected by time-resolved spectra in the $^5D_0 \rightarrow {}^7F_1$ region. Because the symmetry of the sites occupied by surface Eu^{3+} ions is lower, the $^5D_0 \rightarrow {}^7F_1(E)$ line, which is doubly degenerate in the bulk crystal, is split, and the fluorescence lifetime becomes shorter. The results of the laser-selective excitation indicate that the degradation of the site symmetry of Eu^{3+} seems to be abrupt, which means the as-synthesized $La_2O_2S:Eu^{3+}$ NCs might be of the $La_2O_2S/La_2O_{2-x}S_{1+x}$ core−shell structure and the shell are not in a disordered state but a rather pure one.

1. Introduction

In recent years, trivalent europium (Eu^{3+})-doped nanosized oxide phosphors have attracted great interest due to their potential application in high-resolution displays and their unique physical properties distinctive to the bulk.[1−5] As an efficient red light phosphor, however, Eu^{3+}-doped oxysulfide nanocrystals (NCs) were given rather little attention. The reason might be that the oxysulfide NCs could not be prepared easily.

Obtaining bulk $Ln_2O_2S:Eu^{3+}$ (Ln = La,Y) with good quality is not an easy task. The conventional way is a solid-state reaction by the reaction of yttrium and europium oxide with elemental sulfur and reflux ($Na_2CO_3/K_3PO_4/Na_2S_2O_3$) at high temperature.[6−12] There are other methods, such as the sulfuration of rare earth oxides by H_2S or CS_2,[13] the combustion method,[14] and the solvothermal pressure relief method.[15] When it comes to $Ln_2O_2S:Eu^{3+}$ NCs, the task becomes more troublesome, and the corresponding reports are few. Dhanaraj et al. had reported a two-step solution−gel polymer thermolysis method to synthesize $Y_2O_2S:Eu^{3+}$ NCs.[16] In this method, sodium thiosulfate ($Na_2S_2O_3$) was used to sulfurize the first synthesized $Y_2O_3:Eu^{3+}$ NCs. But the introduction of sodium impurities might influence the luminescent properties of Eu^{3+}. Bang et al. reported the fabrication of $Ln_2O_2S:Eu^{3+}$ (Ln = Y, La, Ga) NCs by the combustion method,[17] where dithiooxamide ($(CSNH_2)_2$) acted as the sulfur source. The disadvantages of this method are that $(CSNH_2)_2$ is expensive and the size of the obtained NCs is too large (100−200 nm). We report in this paper a direct and facile route to fabricate $La_2O_2S:Eu^{3+}$ NCs using gel thermolysis. Thiourea ($CS(NH_2)_2$) was employed as the sulfuration source, which was a common chemical reagent and brought no impurity into the NCs. Poly(vinyl alcohol) (PVA) was used as the dispersing medium to limit the agglomeration of the NCs.[18] The final resulting $La_2O_2S:Eu^{3+}$ NCs were determined to be 18 nm with hexagonal morphology.

As is well-known, one of the important properties in nanosized materials is the surface effect originating from the high surface/volume ratio. Under the surface effect, the structure of the surface or its vicinity is in a disordered state. It should be remarked that ions on the surface and near the surface are both regarded as surface ions in the following. When approaching the surface from the interior, there should be a step-by-step declining process of local symmetry. The Eu^{3+} ion is sensitive to the surrounding environment, and the degradation of the crystal field (CF) will cause shifts and splittings of CF levels. Through the use of Eu^{3+} as a probe, the degrading process could be detected. In our previous work, only a new broad excitation line at 579.9 nm was observed in $Y_2O_3:Eu^{3+}$ NCs, where Eu^{3+} occupies C_2 site symmetry.[19] In $YVO_4:Eu^{3+}$ NCs, where Eu^{3+} occupies D_{2d} site symmetry at the particle center, the gradual splitting process of the CF levels was reported by our coresearchers.[20] The higher the symmetry of the bulk, the clearer the degradation process in the NCs. Therefore, it is expected that in $La_2O_2S:Eu^{3+}$ NCs the symmetry degradation process should be vividly manifested because of the C_{3v} site symmetry Eu^{3+} occupied. In this work, time-resolved spectra and laser-selective excitation experiments were performed on the as-synthesized sample to study the surface effect.

2. Experimental Section

2.1 Synthesis of $La_2O_2S:Eu^{3+}$ NCs. In this paper, $La_2O_2S:Eu^{3+}$ NCs were fabricated by gel thermolysis. During the thermolysis reaction, thiourea acted as the sulfur source for $La_2O_2S:Eu^{3+}$; it was also employed as the fuel to provide enough heat for the reaction. To prevent the agglomeration of the $La_2O_2S:Eu^{3+}$ particles, PVA was used as a dispersing agent. The thermolysis reaction to synthesize $La_2O_2S:Eu^{3+}$ NCs could be written as the following

$$a[(1-x)La(NO_3)_3 + xEu(NO_3)_3] + b[CS(NH_2)_2] + c[PVA] \rightarrow a/2[(La_{1-x}Eu_x)_2O_2S] + \text{byproducts}$$

where *c*:*b*:*a* was the molar ratio of the network to the fuel to

* Author to whom correspondence should be addressed. E-mail: hillphs@sina.com.
† Beijing Jiaotong University.
‡ Chinese Academy of Science.
§ University of Science and Technology, Beijing.

10.1021/jp0453414 CCC: $30.25
Published on Web 02/26/2005

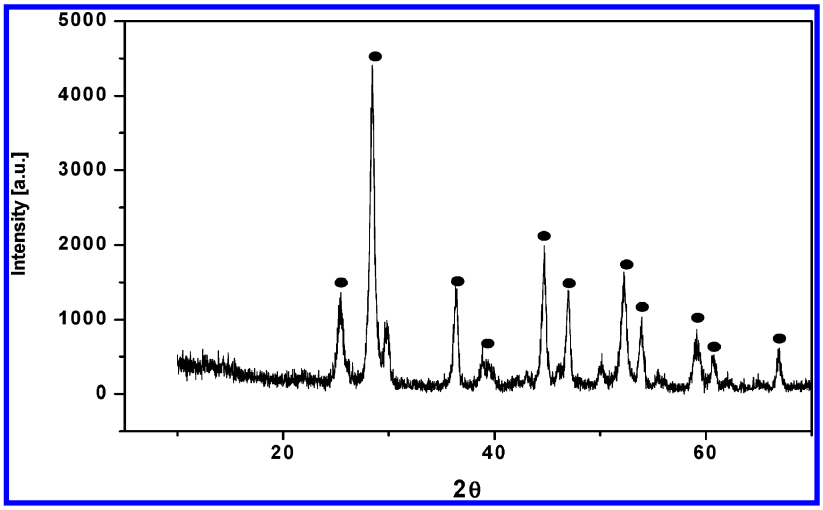

Figure 1. X-ray diffraction pattern of $La_2O_2S:Eu^{3+}$ NCs (● indicates La_2O_2S phase).

the oxidizer and the byproducts might be the mixture of CO_x, SO_x, NO_x, and H_2O produced in the reaction with an adequate supply of oxygen and a sufficiently high temperature.

First, $(La/Eu)(NO_3)_3$ stock solutions were respectively obtained by dissolving the corresponding oxides (99.99% purity) in dilute nitric acid (analytic reagent). Then the solutions were mixed with the molar ratio of Eu/La 4%, and the acidic pH is adjusted to approximately pH 5 by adding dilute ammonia solution. With the consideration that $CS(NH_2)_2$ provides sulfur for the formation of $La_2O_2S:Eu^{3+}$ and PVA influences the size of the NCs, $CS(NH_2)_2$ (analytic purity) solution and PVA solution were added quasi-empirically to this solution. After being stirred for 30 min at 80 °C with a magnetic stirrer, the solution was evaporated in a crucible, and a gel resulted. Subsequently, the gel was dehydrated in an infrared desiccator for 2 h and thermolyzed in air at 300 °C for a few minutes. Then the white powder product in the crucible was collected and annealed at 500 °C for an hour to remove the organic components. The $La_2O_2S:Eu^{3+}$ NCs were at last obtained, and the measurements were performed.

2.2. Characterization. The purity, structure, size, and morphology of the as-synthesized $La_2O_2S:Eu^{3+}$ NCs were, respectively, characterized by X-ray powder diffraction (XRD, Rigaku, D/max-RBX, Cu Kα radiation) and by transmission electron microscopy (TEM, JEM-2000FX).

2.3. Optical Measurements. In the measurements, the powder sample was deposited into a dent of a thin aluminum plate airproofed by a glass flake. The plate was then put into a liquid-nitrogen-cooled quartz Dewar. A 355 nm light generated from a pulsed Nd^{3+}:yttrium−aluminum−garnet (YAG) laser (with a repetition rate of 10 Hz and a duration of 10 ns) combined with a third-harmonic generator was used as the excitation source. For the laser-selective excitation experiment, a Powerlite Precision II scientific laser system (composed of a Powerlite Precision II 8000 and a Sunlite EX OPO and FX-1) was used. The emission and excitation spectra were recorded by a spectrometer (Spex 1403), a photomultiplier tube, and a boxcar averager and processed by a computer.

3. Results and Discussion

3.1. Analysis of the NC Fabrication. During the synthesis of the oxysulfide NCs, there are several crucial steps. First, the molar ratio *c*:*b*:*a* should be reasonable. As mentioned in section 2.1, PVA provides the network/cage to limit the growth of the nanoparticles, and $CS(NH_2)_2$ served as the sulfur source. But too high amounts of those will introduce C, H, N, and S into the powder products due to insufficient combustion. By use of an orthogonal experiment, the optimal ratio is chosen as 1.5:1.6−1.8:1. To be of even components, it is necessary for the solution to be stirred at 80 °C. This is helpful for the inorganic ions to penetrate the long PVA chains. Another factor is the annealing temperature. Treatment temperatures as high as 600 °C will convert the oxysulfide into oxysulfate. This may be due to the high surface/volume ratio and the larger surface energy of the NCs, which makes the oxidation easier. So we adopt 500 °C as the annealing temperature. It should be mentioned that the gel could not be directly exposed to the lamp during dehydration in case the sulfur anions may be deoxidized into sulfur.

The XRD pattern of the $La_2O_2S:Eu^{3+}$ NCs sample is shown in Figure 1. In the pattern, the dominant phase is in agreement with JCPDS #27-0263 for La_2O_2S, which crystallizes in the hexagonal $P\bar{3}m1$ space group. Through the use of Sherrier's formula, the average size is determined to be ∼18 nm based on the diffraction line width at the angle of $2\theta = 28.4°$. From TEM images in Figure 2, the average size of the NCs can be further affirmed.

Figure 2 shows the TEM images of $La_2O_2S:Eu^{3+}$ NCs. It can be seen from the images that both well-dispersed and aggregated NCs coexist in the as-synthesized $La_2O_2S:Eu^{3+}$ NCs. Hence, it was proven that the dispersing agent PVA does not work as had been expected. However, PVA does help the formation of nanocrystalline La_2O_2S because there are no NCs, but the bulk one formed without PVA. It is presumed that PVA limits the growth of La_2O_2S particles at the inception of thermolysis. When it comes to the final stage, the network PVA gradually decomposes, and partially agglomerated NCs result due to the residual heat. Therefore, other factors such as homogeneous heat distribution should be further considered to improve the dispersion quality of the NCs.

3.2. Luminescent Properties of $La_2O_2S:Eu^{3+}$ NCs. In bulk $La_2O_2S:Eu^{3+}$, the europium ion (with ion radius 0.98 Å) is expected to occupy the lanthanum (1.14 Å) site because of the slight difference of ionic radius between the two cations. Hence, the local symmetry of the Eu^{3+} site in $La_2O_2S:Eu^{3+}$ is C_{3v}. Both the split of the J ($J = 1-2$) manifolds of $Eu^{3+}$and the

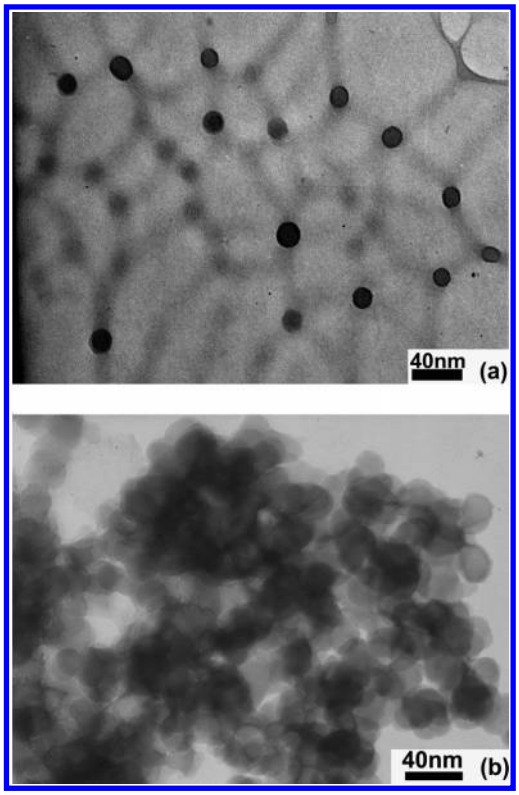

Figure 2. TEM images of (a) well-dispersed and (b) slightly aggregate $La_2O_2S:Eu^{3+}$ NCs.

TABLE 1: Energy Levels of Eu^{3+} in Polycrystalline $La_2O_2S:Eu^{3+}$ (cm^{-1})

levels	IRs	in bulk
$^7F_1$	E	350.8
	A	376.9
$^7F_2$	A	938.4
	E	
	E	1167.3
$^5D_0$	A	17185.9

corresponding irreducible representations (IRs) under C_{3v} symmetry are listed in Table 1, where the data are taken from ref 21.

Figure 3 shows the emission spectrum of $La_2O_2S:Eu^{3+}$ NCs. The main transitions originating from the $^5D_0$ level are marked on the spectrum, from which we can see that both the positions and numbers of the emission lines are in agreement with those of the bulk calculated from Table 1.

Figure 4 shows the time-resolved emission spectra of $La_2O_2S:Eu^{3+}$ NCs. It can be seen clearly from Figure 4a that with a decrease in the delay time a new emission peak appears at the high-energy side of the $^5D_0 \rightarrow {}^7F_1$ lines, which means the emergence of a new luminescent center with a short lifetime. It should be mentioned that there is a remote possibility to attribute the new center to Eu^{3+} ions in the impurities. The energy of the $^5D_0 \rightarrow {}^7F_0$ transition is mainly affected by a nephelauxetic effect. As a consequence, the number of the $^5D_0 \rightarrow {}^7F_0$ lines is equal to the number of different Eu^{3+} sites in the bulk. If the new peak is caused by an impurity, considering the fact that the $^5D_0 \rightarrow {}^7F_1$ line blue shifts, then there must be a corresponding shift of the $^5D_0 \rightarrow {}^7F_0$ emission with a short delay time because of different nephelauxetic effects in different hosts. As a matter of fact, however, the $^5D_0 \rightarrow {}^7F_0$ line keeps rather stable in Figure 4a, which contradicts the previous presumption. Therefore, it is reasonable to assign the new line to the $La_2O_2S:Eu^{3+}$ NCs. Since the $^5D_0 \rightarrow {}^7F_0$ transition is weak in the bulk, they are difficult to resolve even if there are slight changes in the NCs, which is different from the case for impurities. Thus, the number of the $^5D_0 \rightarrow {}^7F_0$ line is no longer an effective criterion to determine the number of Eu^{3+} sites in the NCs.

As we all know, that CT band is a wide-band excitation, so in $La_2O_2S:Eu^{3+}$ NCs the excited Eu^{3+} ions include both the interior ones and the surface ones. We presume that the new peak is caused by surface Eu^{3+} ions. To confirm the above assumption, first, the 468 nm excitation was performed on the NCs, because 468 nm corresponds to the $^7F_0 \rightarrow {}^5D_2$ resonant transition and only the interior Eu^{3+} ions are excited. It is evident in Figure 4b that both the$^5D_0 \rightarrow {}^7F_0$ and the $^5D_0 \rightarrow {}^7F_1$ line positions remain unchanged with a decrease of the delay time, which are the emissions of interior Eu^{3+} ions. Second, from the view of group theory, the 2-fold E level is split into two levels with the declining local symmetry of Eu^{3+}. It is usually assumed that in NCs the site symmetry of the surface Eu^{3+} ions is lower than that of the interior ions under the surface effect. Therefore, one $^5D_0 \rightarrow {}^7F_1$(E) line will be split into two lines. Furthermore, from Table 1, we know that in the bulk the $^7F_1$-(E) level is at the high-energy side of the $^7F_1$(A) level. Hence, in the NCs the new $^5D_0 \rightarrow {}^7F_1$ line should at the high-energy side, which is consistent with the new peak in Figure 4a. Hence, the assumption is confirmed.

Since the $^7F_2$ manifold has two 2-fold E levels under C_{3v} and the $^5D_0 \rightarrow {}^7F_2$ transition is the most prominent transition of Eu^{3+}, the level splitting due to the surface effect should be more clear in the $^5D_0 \rightarrow {}^7F_2$ region. Figure 5 shows the selective

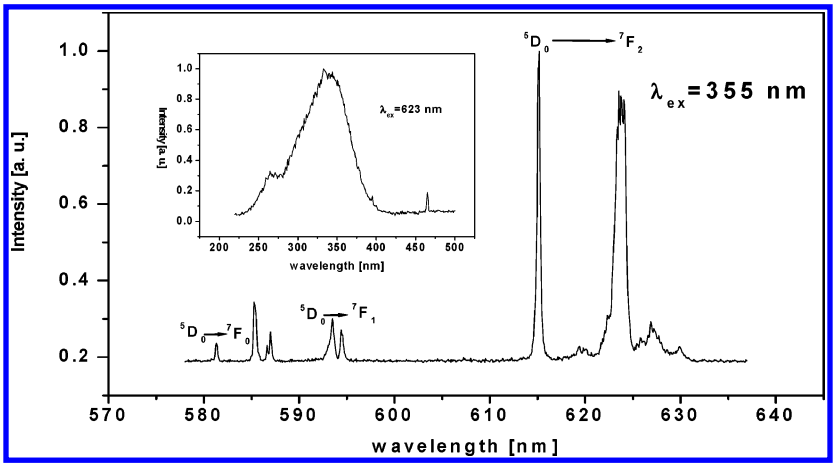

Figure 3. Photoluminescence emission spectrum of $La_2O_2S:Eu^{3+}$ NCs measured at 77 K. The excitation wavelength is 355 nm. The insert is the excitation spectrum measured at room temperature monitored at 623 nm.

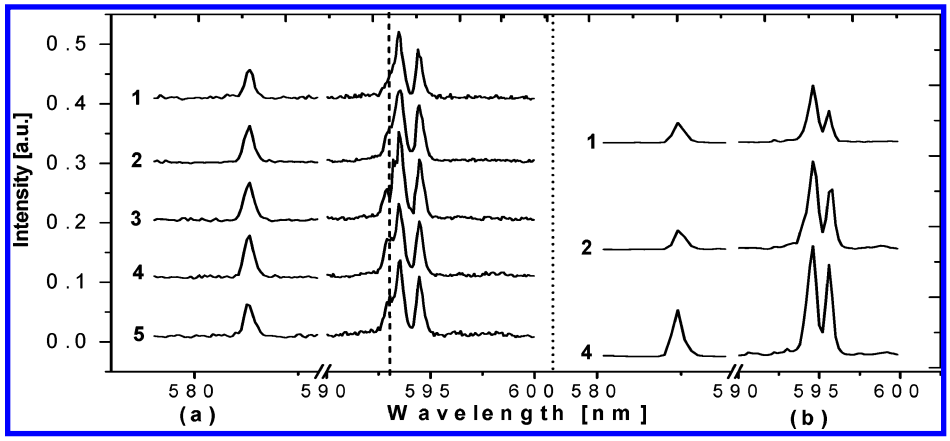

Figure 4. Time-resolved emission spectra of $La_2O_2S:Eu^{3+}$ NCs under different excitations at (a) 355 nm and (b) 468 nm at 77 K. The delay times of the spectra labeled from 1 to 5 are, respectively, 10, 1, 0.2, 0.1, and 0.05 ms. The dashed line in part a indicates the appearance of a new emission peak.

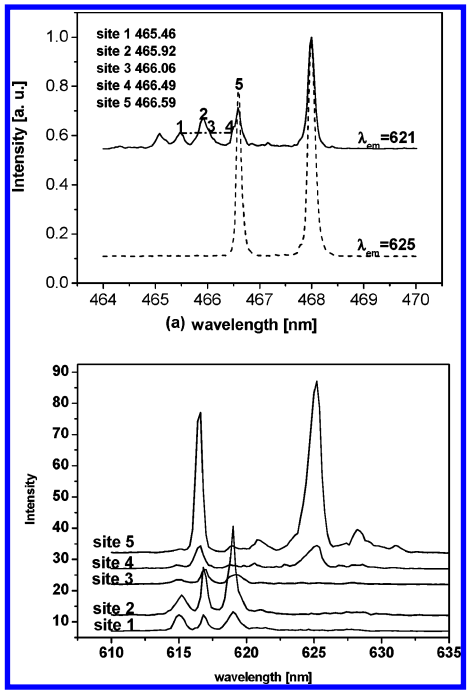

Figure 5. (a) Excitation spectra of $La_2O_2S:Eu^{3+}$ NCs measured at 77 K. The solid line is measured by monitoring a 621 nm light and the dashed line by monitoring a 625 nm light. (b) The emission spectra under various excitation wavelengths were measured at 77 K with a delay of 100 μs. In part a, the excitation sites (from site 1 to 5) are marked on the solid line, and the detailed numerical values are also denoted.

excitation spectra of the $La_2O_2S:Eu^{3+}$ NCs in the $^5D_0 \rightarrow {}^7F_2$ region. In Figure 5b, there is no substantial difference between the emission spectra under excitation of site 1 and 2, and the spectrum under site 5 is like that of the bulk. When excited from site 1 (or 2) to site 3, 4, and 5, the 615 and 619 nm lines are weakened and disappear with the simultaneous emergence of a 625 nm line.

We know that the relative intensities of the emission lines originating from the same luminescent center will remain constant under different excitations; therefore, it is reasonable to assign the 615, 616.7, and 619 nm lines to the Eu^{3+} site rather than C_{3v}. There exist two possibilities for the origin of the new site. One is that it comes from the Eu^{3+} ions (site A) in the impure phase; the other is that it comes from the surface Eu^{3+} ions in the $La_2O_2S:Eu^{3+}$ NCs. For the former, it seems that the assignment could be confirmed by the impure phase in the XRD pattern in Figure 1. But if it is true, where are the surface Eu^{3+} ions? And the relative emission intensity of site A to that of the NCs should bear a resemblance to the relative X-ray diffraction intensity of the impure phase of the NCs. However, no emission of site A is observed under the 355 nm excitation, even with a short delay time. Therefore, the latter assignment seems to be the most likely one. Since the evolution process of the surface Eu^{3+} site is abrupt, it means that there is no transition from the interior to the surface in the oxysulfide NCs and the lower symmetry of the surface is in a rather pure state. This contradicts the common assumption that the transition from the interior to the surface is gradual in nanocrystals, which has been confirmed in the $YVO_4:Eu^{3+}$ system.[20] We suggest that the surface state varies with the system and synthesis method. In our case, the initial oxysulfide crystallizes according to the stoichiometric component of La_2O_2S under ample oxygen and sulfur atmosphere. At the final stage of growth, the sulfur is not sufficient in comparison to the ambient oxygen atmosphere, and the sulfur anions are inclined to be oxidized due to the high surface energy. Thus, the component of the outer layer of the NCs grows with the tendency of $La_2O_{2-x}S_{1+x}$. In another words, the as-synthesized sample has the $La_2O_2S/La_2O_{2-x}S_{1+x}$ core−shell structure. It should be mentioned that the core−shell structure still needs further confirmation, and this will be the emphasis of our work in the future.

4. Conclusions

The $La_2O_2S:Eu^{3+}$ NCs are prepared by gel thermolysis. The molar ratio of $RE(NO_3)_3/CS(NH_2)_2/PVA$ is determined to be 1.5:1.6−1.8: 1, and the annealing temperature is 500 °C. The average size of the NCs is 18 nm.

Through the use of time-resolved spectra, surface Eu^{3+} ions are first detected in the $^5D_0 \rightarrow {}^7F_1$ region. A new peak with a shorter lifetime appears in the high-energy side of the $^5D_0 \rightarrow {}^7F_1(E)$ line of the interior Eu^{3+} ions under the surface effect. According to laser-selective excitation and emission, two luminescent centers are resolved in the sample. One is the C_{3v} site symmetry of the interior Eu^{3+} ions; the other is the lower site symmetry occupied by surface Eu^{3+} ions. Because of the abrupt transition from the interior to the surface, the $La_2O_2S:Eu^{3+}$ NCs are thought to have the $La_2O_2S/La_2O_{2-x}S_{1+x}$ core−shell structure.

Acknowledgment. This work was supported by the Excellent Doctor's Science and Technology Innovation Foundation of Beijing Jiaotong University (48001), the National Natural

Science Foundation of China (10374002), and the State Key Project of Basic Research (2003CB314707).

References and Notes

(1) Eilers, H.; Tissue, B. M. *Chem. Phys. Lett.* **1996**, *74*, 251.
(2) Meltzer, R. S.; Feofilov, S. P.; Tissue, B.; Yuan, H. B. *Phys. Rev. B* **1999**, *60*, R14012.
(3) Igarashi, T.; Ihara, M.; kusunoki, T.; Ohno, K.; Isobe, T.; Senna, M. *Appl. Phys. Lett.* **2000**, *76*, 1549.
(4) Wakefield, G.; Holland, E.; Dobson, P. J.; Hutchison, J. L. *Adv. Mater.* **2001**, *13*, 1557.
(5) Peng, H. S.; Song, H. W.; Chen, B. J.; Wang, J. W.; Lu, S. Z.; Kong, X. G.; Zhang, J. H. *J. Chem. Phys.* **2003**, *118*, 3277.
(6) Eick, H. A. *J. Am. Chem. Soc.* **1958**, *80*, 43.
(7) Kanehisa, O.; Kano, T.; Yamamoto, H. *J. Electrochem. Soc.* **1985**, *132*, 2023.
(8) Morell, A. *J. Electrochem. Soc.* **1991**, *138* (14), 1100.
(9) Kottaisamy, M.; Jagannathan, R. *J. Electrochem. Soc.* **1995**, *142* (9), 3205.
(10) Chang, S. Y.; Choi, Q. W.; Choi, H.; Mho, S. I. *J. Solid State Inorg. Chem.* **1996**, *133*, 1123.
(11) Kottaisamy, M.; Horikawa, K.; Kominami, H.; Aoki, T.; Azuma, N.; Nakamura, T.; Nakanishi, Y.; Hatanaka, Y. *J. Electrochem. Soc.* **2000**, *147*, 1612.
(12) Lo, C. L.; Duh, J. G.; Chiou, B. S.; Peng, C. C.; Ozawa, L. *Mater. Chem. Phys.* **2001**, *71*, 179.
(13) Haynes, J. W.; Brown, J. J. *J. Electrochem. Soc.* **1968**, *115*, 1060.
(14) Mishenina, L. N.; Kazarbina, T. V.; Kozik, V. V. *Inorg. Mater.* **1994**, *30*, 733.
(15) Yu, S. H.; Han, Z. H.; Yang, J.; Zhao, H. Q.; Yang, R. Y.; Xie, Y.; Qian, Y. T.; Zhang, Y. H. *Chem. Mater.* **1999**, *11*, 192.
(16) Dhanaraj, J.; Geethalakshmi, M.; Jagannathan, R.; Kutty, T. R. N. *Chem. Phys. Lett.* **2004**, *387*, 23.
(17) Banga, J.; Abboudib, M.; Abramsa, B.; Holloway, P. H. *J. Lumin.* **2004**, *106*, 177.
(18) Dhanaraj, J.; Jagannathan, R.; Kutty, T. R. N.; Lu, C. H. *J. Phys. Chem. B* **2001**, *105*, 11098.
(19) Peng, H. S.; Song, H. W.; Chen, B. J.; Lu, S. Z.; Huang, S. H. *Chem. Phys. Lett.* **2003**, *370*, 485.
(20) Yan, C. H.; Sun, L. D.; Liao, C. S.; Zhang, Y. X.; Lu, Y. Q.; Huang, S. H.; Lu, S. Z. *Appl. Phys. Lett.* **2003**, *82*, 3511.
(21) Sovers, O. J.; Yoshioka, T.*J. Chem. Phys.* **1969**, *51*, 5330.